



Article

# A Novel Rotor Harmonic Winding Configuration for the Brushless Wound Rotor Synchronous Machine

Farhan Arif <sup>1,†</sup>, Arsalan Arif <sup>2,\*,†</sup>, Qasim Ali <sup>3</sup>, Asif Hussain <sup>4</sup> , Abid Imran <sup>2</sup>, Mukhtar Ullah <sup>1</sup> and Asif Khan <sup>5,\*</sup>

<sup>1</sup> Department of Electrical Engineering, FAST National University of Computer and Emerging Sciences, Islamabad 44000, Pakistan; mukhtar.ullah@nu.edu.pk (M.U.)

<sup>2</sup> Faculty of Mechanical Engineering, Ghulam Ishaq Khan Institute of Engineering Sciences and Technology, Islamabad 23460, Pakistan; abid.imran@giki.edu.pk

<sup>3</sup> Department of Electrical Engineering, Sukkur IBA University, Sukkur 65200, Pakistan; qasim-ali@iba-suk.edu.pk

<sup>4</sup> Department of Electrical Engineering, University of Management and Technology, Lahore 54782, Pakistan

<sup>5</sup> Mechanical Engineering Program, Physical Science and Engineering Division, King Abdullah University of Science and Technology (KAUST), Thuwal 23955-6900, Saudi Arabia

\* Correspondence: arsalan.arif@giki.edu.pk (A.A.); asif.khan@kaust.edu.sa (A.K.)

† These authors contributed equally to this work.

**Abstract:** In the last decade, permanent magnet (PM)-free or hybrid PM machines have been extensively researched to find an alternative for high cost rare-earth PM machines. Brushless wound rotor synchronous machines (BL-WRSMs) are one of the alternatives to these PM machines. BL-WRSMs have a lower torque density compared to PM machines. In this paper, a new topology is introduced to improve the torque producing capability of the existing BL-WRSM by utilizing the vacant spaces in the rotor slots. The new topology has two harmonic windings placed on the rotor which induce separate currents. A capacitor is used between the two harmonic windings to bring the currents in phase with each other. The harmonic winding currents are fed to the rectifier which is also placed on the rotor. Due to additional harmonic winding, the overall field current fed to the rotor field winding has been increased and hence the average torque has also increased. Finite element analysis (FEA)-based simulations are performed using ANSYS Maxwell to validate the proposed topology. The results show that the average torque of the machine has been significantly increased compared to the reference model. The detailed comparison results are provided in this paper.

**Keywords:** synchronous machine; wound rotor; brushless excitation; harmonic excitation



**Citation:** Arif, F.; Arif, A.; Ali, Q.; Hussain, A.; Imran, A.; Ullah, M.; Khan, A. A Novel Rotor Harmonic Winding Configuration for the Brushless Wound Rotor Synchronous Machine. *World Electr. Veh. J.* **2024**, *15*, 226. <https://doi.org/10.3390/wevj15060226>

Academic Editor: Joeri Van Mierlo

Received: 2 April 2024

Revised: 10 May 2024

Accepted: 14 May 2024

Published: 23 May 2024



**Copyright:** © 2024 by the authors. Licensee MDPI, Basel, Switzerland. This article is an open access article distributed under the terms and conditions of the Creative Commons Attribution (CC BY) license (<https://creativecommons.org/licenses/by/4.0/>).

## 1. Introduction

Electric vehicles (EVs) are environmentally friendly, and thus, a considerable amount of research has been conducted to improve the equipment used in EVs [1]. These vehicles face some low-speed road conditions; it is necessary to drive the machine to maintain a stable torque at low speeds. Permanent magnet synchronous machines (PMSMs) for EVs studied in [2] and the cogging torque along with the dynamic performance of the PMSMs at different skew angles were investigated. The stator skew slot was often adopted to reduce torque ripple; however, it declined the output torque at same time. In addition, the differences between a positive rotation performance and a negative rotation performance caused by the skew slot were often ignored. Ever since the advent of high-energy permanent magnet (PM) materials, research on PM machines has gained considerable attention, and this area of continues to increase in popularity. The permanent magnet vernier machines (PMVMs) are a promising solution for low-speed, direct-drive applications, which make them good candidates to be used in EVs. A dual-stator interior permanent magnet vernier machine (DS-IPMVM) was investigated in [3], where the magnets were aligned perpendicular to the air gap, and the two stators were shifted by one half-slot pitch. The useful

magnet flux was improved in this design, thereby achieving a higher torque density, higher flux density and higher power factor, along with a lower cogging torque and less magnet volume compared to the conventional DS-SPMVM. Furthermore, suitable current vector control was used to obtain a larger electromagnetic torque. Typically, PMVMs feature a significantly higher number of rotor pole pairs in comparison to stator pole pairs, along with higher operating frequencies compared to conventional machines. The high operating frequency results in high reactance of the machine, leading PMVMs to have a low-power factor [4]. Hence, a high rating inverter is generally required to drive the machine.

Permanent magnet synchronous machines have also been a prominent area of research for the industrial market due to their high-quality performance. The applicable machine structure along with the drive system becomes costly, mainly due to the use of PMs in applications where the product cost is a main concern. In recent years, wound rotor synchronous machines (WRSMs) have been investigated as an alternative to PM machines. Due to their less expensive structure and wide speed range capabilities, which offer a degree of freedom for flux weakening comparable to that of PM machines, they have gained popularity in variable speed applications. Some of the recent advancements have been in exploiting the power density limits of interior permanent magnet synchronous machines (IPMSMs) [5,6]. In particular, the wide speed range operation of IPMSMs has been specifically investigated for use in electric vehicles and other variable speed applications. Flux controllability for vernier machines for direct-drive applications has been discussed in [7]. The machine was operated for wide speed ranges, achieving a high torque output at low-speed operation and flux weakening control at high-speed operation. In [8], a consequent-pole hybrid vernier machine was proposed by combining the hybrid excited concept and vernier structure, and the consequent-pole magnet arrangement was employed on the outer rotor to achieve a high torque density at low speed and flux weakening capability at high speed, making it attractive for electric vehicle applications. The direct current field windings were mounted between modulating poles, which helped to increase the space utilization ratio and enabled flux regulation without decreasing torque capability. The flux weakening technique for PM machines was experimentally validated using winding switching in [9]. Two different speed ranges were achieved by changing the polarity of the winding coils on the stator of the machine, enabling the machine to operate at a speed beyond the winding switching point. Furthermore, the constant torque region of the machine was extended, and the output power capability was also enhanced.

Different hybrid excited machines were reviewed in [10] on the basis of PMs and direct current (DC) excitation location, as well as the series/parallel connection of PMs and DC excited magnetic fields, respectively. The flux weakening was compared with different control strategies, and the advantages and drawbacks of each category were also analyzed. A major issue with PM machines is the high cost of rare-earth PMs. The availability of these materials is also a huge concern, and complex control for a wide range of speed operations adds to the challenges.

The major rise in the price of PM materials drives the search for alternatives in traction applications like EVs; so, magnet-less machines are being widely regarded as potential alternatives. The permanent magnet vernier machine is a good candidate for EVs as it produces almost double the back EMF compared to conventional permanent magnet synchronous machines. A wound field pole changing vernier machine with a fractional slot concentrated winding for electric vehicles was investigated in [11], utilizing the advantages of a PM and electromagnet in a single topology using a fractional slot concentrated armature winding. The machine operated in a vernier mode at low speeds and a WRSM mode at high speeds. A brushless wound rotor vernier machine for variable speed applications was proposed in [12], where brushless operation was achieved by generating and utilizing the third harmonic component. An additional armature winding was placed on the stator in order to achieve brushless operation.

In the conventional wound rotor vernier machine (WRVM), a third-harmonic current is generated by connecting a 4-pole armature and 12-pole excitation windings in series with a

3-phase diode rectifier in order to generate a pulsating field in the air gap. However, in [13], the armature winding was supplied by a three-phase current source inverter, whereas the auxiliary winding was kept open. The generated fundamental MMF component in the air gap created a four-pole stator field, while the third-harmonic MMF induced the harmonic current in the rotor harmonic winding, generating torque with low ripples due to the open-circuited winding pattern. In recent years, WRSMs have been investigated as an alternative, owing to the cheaper structure manufacturing and wide speed range capabilities given the degree of freedom for flux weakening, which is comparable to that of the PM machines. Ref. [14] suggested that the conventional wound field synchronous machine could be competitive with permanent magnet traction motors. It was specifically demonstrated that field weakening through field current control can result in more efficient operation at high speeds where the machine operates in a traction vehicle application most of the time. From further analysis, it was suggested that the conventional WRSM could be a viable alternative to a PMSM in electric vehicle applications. While comparing different parameters of conventional WRSMs with PMSMs, the WRSM has great advantages in terms of a low-cost rotor which requires only copper winding, core and field current for its excitation, three control variables ( $i_d$ ,  $i_q$  and  $i_f$ ) allow the extended control of the WRSM for a wide speed range, and the machine cost is not related to the cost of the PM material. The authors in [15] investigated some basic synchronous machine designs, compared the performance to a brushless permanent magnet machine of a similar size and discussed the potential of using a wound rotor synchronous machine in an automotive drive application. Additionally, a PM-less rotor exhibits no PM loss; the machine features improved safety through direct field control during inverter fault conditions and there is no problem of de-magnetization. There has been some research conducted for the brushless topologies for WRSMs.

However, WRSM has an inherent problem regarding the assembly of brushes and slip rings. Because of the problem associated with WRSM, a comparative investigation always favors the use of a PMSM instead of WRSM in many applications. To address the aforementioned problems, many brushless excitation techniques have been proposed for WRSMs. One solution is generating harmonic flux in the air gap along with fundamental flux to induce voltage in an additionally provided winding on the rotor which is connected to the field winding of the rotor through a rectifier for brushless excitation [16,17]. Multiphase electric machines have benefits of fault tolerance and less power electronic switch ratings per phase, and these machines are capable of controlling the multiple air-gap fields independently with differing numbers of pole pairs. A multiphase electric machine has been designed in [18] with windings such that it can control the magnitude and location of multiple air gap magnetic fields, each with a different number of pole pairs, demonstrating its utility for a wide range of applications. A brushless WRSM (BL-WRSM) featuring a concentrated winding was presented in [19] with 36 slots and 48 poles. This configuration generated both the fundamental component and a prominent sub-harmonic component of the magneto-motive force (MMF). To enable brushless operation, an additional winding, termed the excitation winding, was incorporated into the rotor connected to the main field winding through a rectifier.

An almost similar machine was simulated for dual-speed operation at 46 rpm and 1370 rpm in [20], achieving the desired torque at both speeds, but its performance was lagging behind that of the conventional WRSM. However, the avoidance of brushes was the advantage of this machine, which ultimately led to a reduction in sparking, noise and maintenance costs. Alternatively, special stator winding designs have also been investigated in the literature for generating a sub-harmonic component of the air gap flux with either single or dual inverter schemes [21,22]. A brushless excitation system for externally excited synchronous machines was discussed in [23] by replacing slip rings with a full-bridge active rectifier, with a controller mounted on the rotor. The AC signal induced from the stator was used for the rotor DC link, providing the DC current for the rotor excitation. An inverter configuration was designed in [24] to produce a supplementary third-harmonic

element in conjunction with the primary current component to enable brushless operation in a wound field synchronous machine (WFSM). A technique involving the control of time-harmonic magneto-motive force for implementing harmonic current field excitation in a wound rotor synchronous machine (WRSM) was investigated in [25]. The investigated topology did not require varying current magnitudes, extra switches between the inverter and armature winding, complex inverter setups or structural changes to the machine. A method was introduced in [26] to find a good machine design for a brushless electrically excited synchronous machine (BEESM). In this paper, different methods were used to break down the mathematical problem, out of which the best solution was picked saving time due to better optimization efficiency. An optimized LQR strategy was employed for the wound rotor synchronous machine at variable speeds, with variable output applications with enhanced efficiency [27]. For safe power supply to the loads, the machine only operated in the generating mode, providing good flexibility in operation of the synchronous machine, and was suitable for usage in small hydropower and wind generation applications. The two inverters were replaced by single inverter in [28], thereby proposing brushless topology in order to generate an additional sub-harmonic magneto-motive force component. A special stator winding, comprised of two sets of series-connected windings with an unequal number of turns, was used in [28] in order to generate an additional spatial sub-harmonic component in the stator MMF. This additional sub-harmonic MMF component was used for exciting the field winding of the BL-WRSM. The advantage of the proposed brushless topology was the use of a single inverter compared to a dual inverter used in previous studies. For the rotor, there were two separate windings: a harmonic winding and a field winding. Both the harmonic and field windings were connected in parallel with each other over a rotating rectifier. The additional sub-harmonic MMF component generated a rotating air-gap magnetic field, which induced the voltage in the harmonic winding. This induced voltage was then rectified and used to supply a dc current to the field winding.

## 2. Topology and Working Principle

In this paper, the brushless topology of [28] has been utilized in which the sub-harmonic BL-WRSM was introduced with single inverter topology. The stator has ABC and XYZ winding. Both ABC and XYZ windings are connected in series and excited by a single three-phase inverter. The number of turns for ABC windings are double compared to XYZ winding. The reason behind this unique feature is to develop a stator MMF which generates two dominant components, i.e., a fundamental component and a sub-harmonic component. The rotor has two different windings, a field winding and a harmonic winding. The harmonic winding is used to induce the sub-harmonic MMF component of the stator, which is then rectified by a rotating rectifier (placed on the rotor) and the rectified DC field current is fed to the field winding on the rotor to generate torque. The topology and machine layout of [28] are shown in Figure 1.

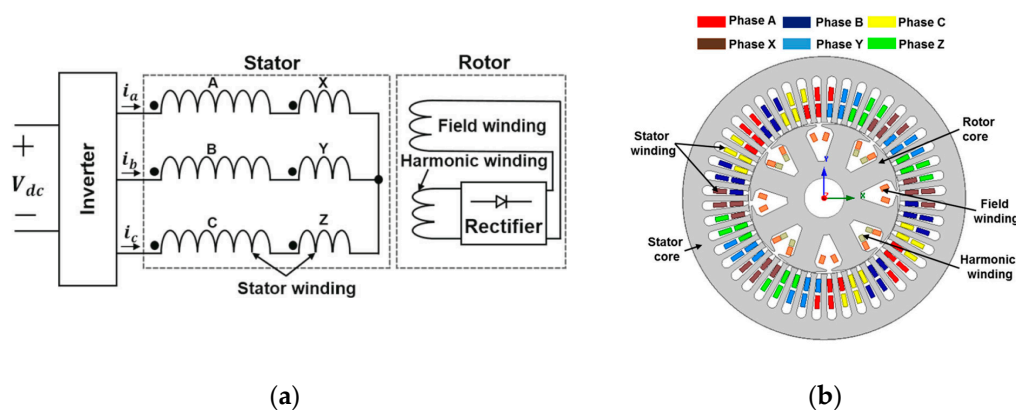


**Figure 1.** Single-inverter excited brushless topology: (a) machine topology and (b) layout.

The stator three-phase windings are excited by three-phase armature currents, which can be represented as

$$\begin{aligned} I_a &= I_m \sin(\omega_e t) \\ I_b &= I_m \sin(\omega_e t - \frac{2\pi}{3}) \\ I_c &= I_m \sin(\omega_e t + \frac{2\pi}{3}) \end{aligned} \tag{1}$$

where  $I_m$  is the peak current supplied by the inverter,  $\omega_e$  is the angular frequency and  $t$  is the time. This current will flow in both the ABC winding and XYZ winding as both of them are connected in series. But, as the number of turns are double for the ABC winding compared to the XYZ winding, the MMF generated by both of them will be different. Here, the brushless topology is designed for 8-pole and 48-slot stator. To elaborate the different harmonic contents, present in the stator MMF due to the specially designed double-layer distributed winding, consider the case, where the phase A current has the maximum amplitude (phase A = 6.4 A, phase B = -3.2 A and, phase C = -3.2 A;  $\omega_e * t = 90$  degrees), and the number of turns in the ABC and XYZ winding are 40 and 20, respectively. The MMF from 0 to 90 and from 180 to 270 mechanical degrees is generated by the XYZ winding, and the MMF from 90 to 180 and from 270 to 360 mechanical degrees is generated by the ABC winding. The MMF is plotted in Figure 2. The difference in the amplitude of the MMF stems from the different number of turns in the two windings.

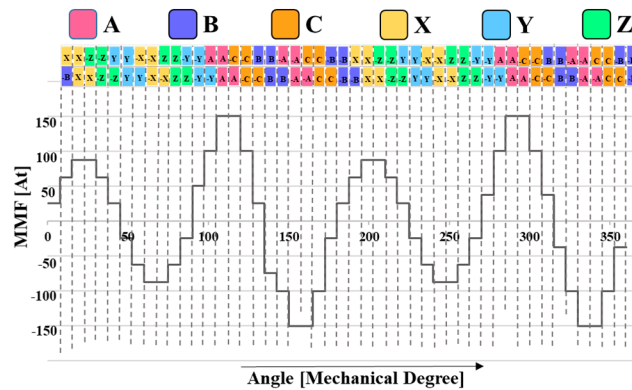


Figure 2. MMF plot of 8-pole, 48-slot stator winding.

Fourier series expansion of this machine’s MMF is shown in Equation (2). The first term (cos function) is the sub-harmonic component used for the excitation of the rotor. The second term (sin function) is the fundamental component of the stator’s MMF. The remaining terms are all of the odd harmonics of the sub-harmonic component and all of the odd harmonics of the fundamental component without the third harmonics.

$$\begin{aligned} F &= -30.9 \cos\left(\frac{\omega_e \times t}{2}\right) + 106.9 \sin(\omega_e \times t) + 17.4 \cos\left(3\frac{\omega_e \times t}{2}\right) + \\ &1.5 \sin(5\omega_e \times t) + 3.6 \cos\left(5\frac{\omega_e \times t}{2}\right) + 1.1 \sin(7\omega_e \times t) + \dots \end{aligned} \tag{2}$$

The angular velocity of the fundamental and the sub-harmonic components is calculated in Equations (3) and (4), respectively. For the fundamental component (8-pole machine with 60 Hz supply and 900 rpm speed), the angular velocity is calculated as

$$\omega_o = \frac{2 \times \pi}{60} \times 900 \text{ rpm} = 94.2 \text{ rad/s} \tag{3}$$

The sub-harmonic component has a different rotating speed from the fundamental synchronous speed, and can be calculated as

$$\omega_h = \frac{\omega_o}{h} = \frac{94.2}{0.5} = 188.5 \text{ rad/s} \tag{4}$$

where  $\omega_h$  is the angular velocity of the harmonic component,  $\omega_o$  is the angular velocity of the fundamental component and  $h$  is the harmonic number (which in this case is 1/2 or 0.5). From these equations, we can conclude that the sub-harmonic component will rotate at a speed twice as high as the fundamental synchronous speed. This different speed helps the harmonic component to become induced in the rotor harmonic winding.

While looking at the machine layout of the existing topology [28], we can notice that the harmonic winding has been housed in half of the rotor slots. The reason for this configuration is that, for the topology to work properly, the harmonic winding needs to be a four-pole winding so that it can induce the sub harmonic, four-pole component of the air gap MMF. The field winding is present in all 8 slots as it needs to be an 8-pole winding so that it matches the main 8-pole component of the air gap MMF.

In this paper, a new topology for the rotor harmonic winding is proposed where the unutilized rotor slots of [28] are being used. For this, a second phase of the harmonic winding is placed in the unutilized 4-pole slots. This second phase of the harmonic winding is identical to the first phase of the harmonic winding, with same number of turns and poles. The proposed topology and its machine layout are shown in Figures 3 and 4. The two phases of the harmonic winding are connected in a series configuration in order to add up the voltages from the two phases and are then rectified by the rotating rectifier before feeding the DC current to the field winding. The proposed topology has been implemented for an 8-pole, 48-slot machine, as shown in Figure 4. The machine parameters are given in Table 1. The machine parameters are kept the same as in [28] so that a fair comparison is drawn from the simulated results.

The rotor with 8-slots but two different windings, the field winding and the harmonic windings, has different pole pitches. The rotor field winding has eight-poles and the harmonic winding has four-poles. The field winding has a pole pitch of one-slot. The harmonic winding has two different phases, H1 and H2, as shown in Figure 5. The pole pitch of the harmonic winding is two slots. In this way, the eight-pole field winding and four-pole harmonic winding have been placed in eight rotor slots.

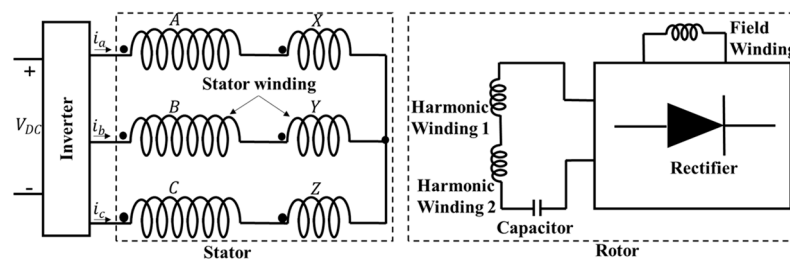


Figure 3. Proposed machine topology.

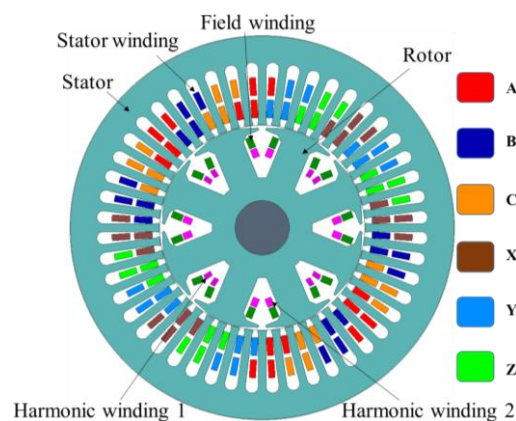
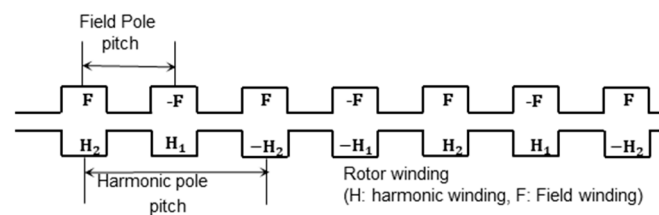


Figure 4. Proposed machine layout.

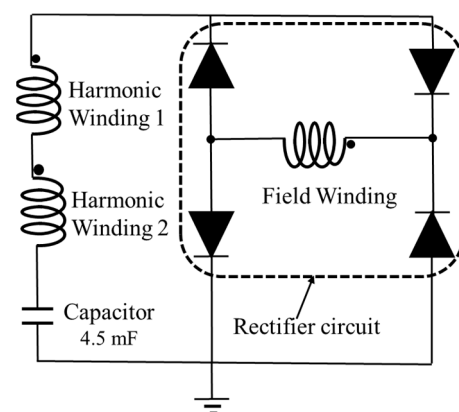
**Table 1.** Specifications of proposed BL-WRSM.

Parameters	Value
Quantity of poles	8
Quantity of stator slots	48
Winding ABC, conductors per stator slot	40
Winding XYZ, conductors per stator slot	20
Field winding, conductors per pole	50
Harmonic winding, conductors per pole	48
Rated power (kW)	1
Operating speed (rpm)	900
Outer diameter of stator (mm)	177
Inner diameter of stator (mm)	95
Diameter of shaft (mm)	25
Length of air gap (mm)	0.5
Stack length (mm)	80

**Figure 5.** Pole pitches of 8-pole field and 2-pole harmonic windings of rotor.

The field winding has half the pole pitch compared to the harmonic winding.

The rotor field winding, two-phase harmonic windings and rotating rectifier connection circuit are shown in Figure 6. The two windings are connected in series and a capacitor is installed in series with them which helps to reduce the voltage pulsations.

**Figure 6.** The rectifier circuit with the field and two-phase harmonic windings and the capacitor.

### 3. FEA Analysis and Results

The machine model and topology introduced in the previous section are simulated in 2-D Ansys Maxwell software which is based upon finite element analysis (FEA). The results have been compared with the already existing topology of [28]. Both the proposed and existing topology have been provided with three-phase AC currents which are shown in Figure 7.

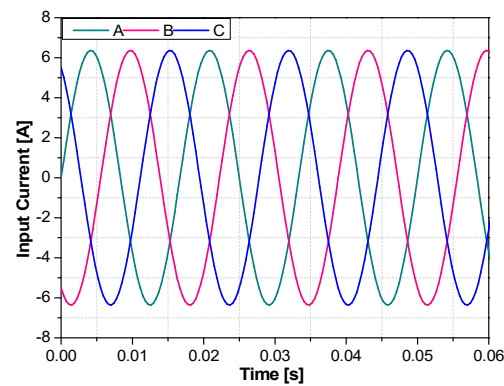
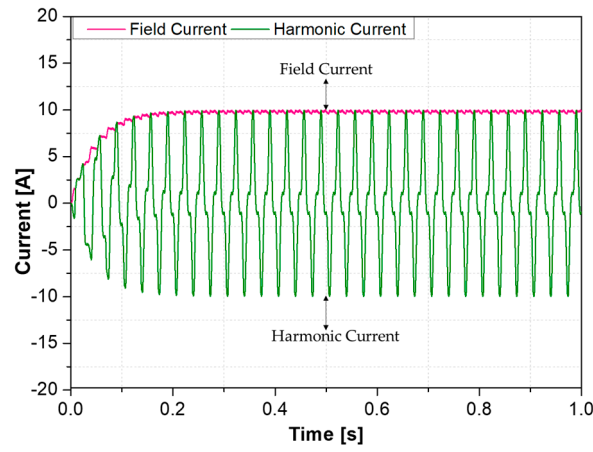


**Figure 7.** Input current to existing topology and proposed topology.

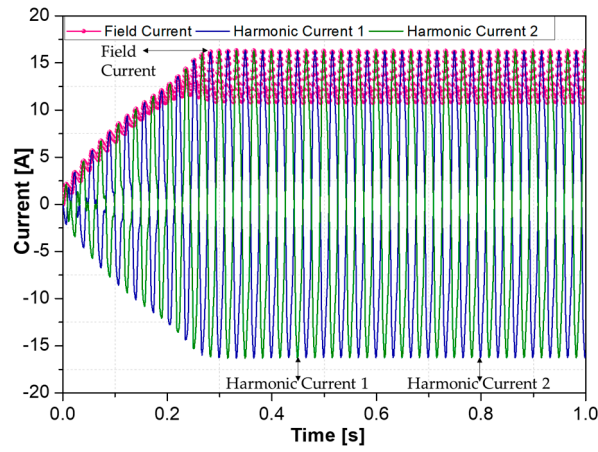
The currents induced in the rotor harmonic windings along with the field winding current fed to the rotor field winding for the existing and proposed topologies are shown in Figure 8. Due to the addition of a second phase of the rotor harmonic winding in the proposed topology, it can be seen that the field winding current has significantly increased, with the ramification that the ripple in the field winding current has also been increased. The average value of the field current in the proposed machine is 9.05 A, while for the proposed brushless machine, the average value of the field current is 12.2 A, which is almost 34% higher. The electromagnetic torque for the existing and proposed topology is plotted in Figure 9. The advantage of the proposed topology can be clearly seen by the improvement in the average torque. The average torque for the proposed topology has been increased by almost 33%. The increase in the torque and field current are almost the same, which points to the fact that for the proposed brushless topology, the output torque is directly proportional to the rectified field current. Along with this increase, the torque ripple has also increased, which is mainly due to the ripples in the field winding current of the proposed topology.

The core loss is illustrated in Figure 10. In the proposed machine, the simulated core loss is 50.77 watts, which is higher as compared to the existing machine. This increase is due to the fact that for the proposed machine, the flux density in the stator as well as the rotor is higher compared to the existing machine, thus leading to elevated core losses. The magnetic flux density plot for the existing and proposed topology is shown in Figure 11. The output of the proposed machine has been clearly increased but from the flux density plot, we can estimate that the proposed machine is performing under the limit of 2 Tesla.

The performance comparison between the existing and proposed topology is summarized in Table 2. The two harmonic windings arranged in a series configuration help to induce a higher harmonic current on the rotor harmonic winding and, in turn, help to increase the field current. The increased field current results in a higher average torque, which is the main advantage of the proposed topology. The copper losses and core losses in the rotor are increased from the existing topology due to the higher rotor currents and rotor flux density, but this does not affect the efficiency to a great extent because of the fact that that torque has increased, which will increase the output power of the machine. In future, rotor shape optimization will be performed regarding the reduction in the torque ripples.

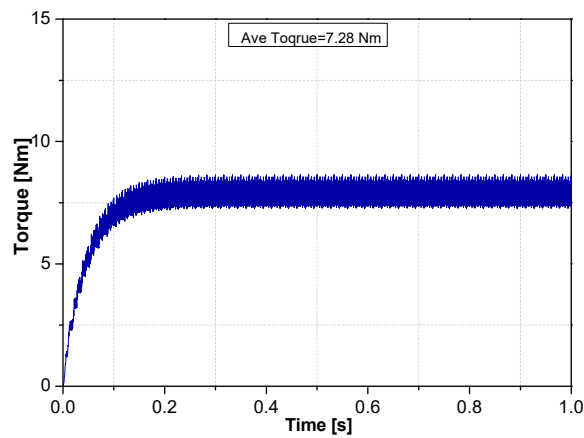


(a)



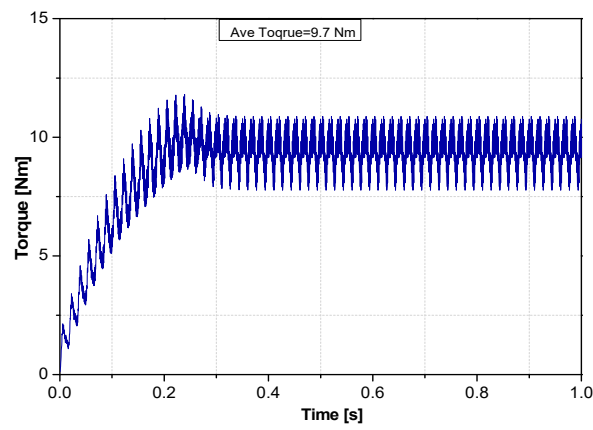
(b)

Figure 8. Induced current in rotor field winding: (a) existing topology; (b) proposed topology.



(a)

Figure 9. Cont.



(b)

Figure 9. Torque: (a) existing topology; (b) proposed topology.

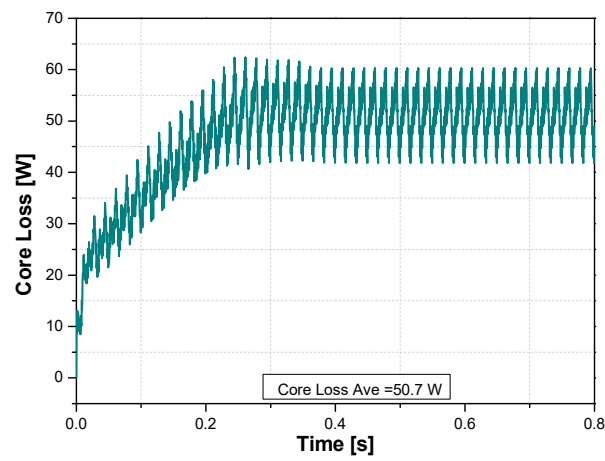
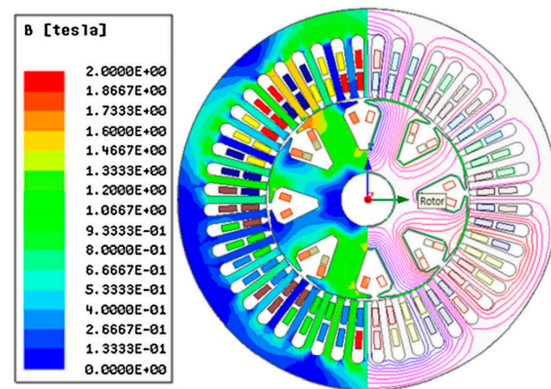
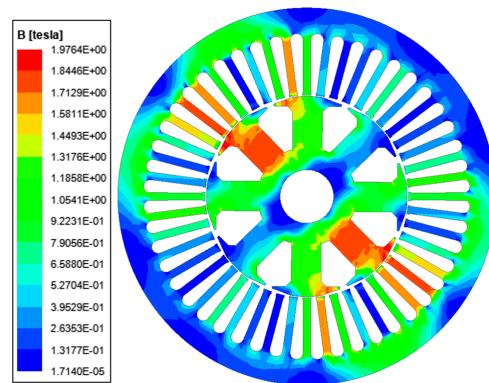


Figure 10. Core loss of proposed topology.



(a)

Figure 11. Cont.



(b)

Figure 11. Magnetic flux density: (a) existing topology; (b) proposed topology.

Table 2. Parameter comparison.

Parameters	Existing Topology	Proposed Topology
Terminal voltage ( $V_{rms}$ )	72.70	87.7
Field current (A)	9.05	12.2
Harmonic current 1 ( $A_{rms}$ )	4.75	11.61
Harmonic current 2 ( $A_{rms}$ )	0	11.61
Stator current ( $A_{rms}$ )	4.5	4.5
Average torque (Nm)	7.28	9.7
Torque ripple (%)	19.13	38.9
Core loss (W)	40.77	50.7
Stator copper loss (W)	68.04	68.14
Field winding copper loss (W)	51.60	93.59
Harmonic winding copper loss (W)	4.06	48.51
Efficiency (%)	80.7	78.2

As the total harmonic distortion (THD) points at the amount of harmonic distortion present in a signal, this measurement gives us information regarding the quality of the machine performance. The THD can be expressed as the ratio of the addition of all harmonic constituents to the fundamental frequency, as shown in the Equation (5).

$$\text{THD} = \frac{V_{\text{RMS without fundamental}}}{V_{\text{RMS fundamental}}} \quad (5)$$

The THD is crucial in the machines industry. In this paper, the THD has been calculated for the stator induced voltage. In order to calculate the THD, fast Fourier transform (FFT) of the current or voltage is required. In that regard, the induced voltage of phase A of the proposed topology is given in Figure 12, and the fast Fourier transform of the induced voltage is shown in Figure 13. The THD of the proposed topology has been calculated as 29% by putting the values of the fundamental and harmonic frequencies into Equation (3). The THD of the proposed topology is a little on the higher side since the THD determines the potential of machine damage. The higher the value of the THD, the greater the risk of damage to the machine. With more distortion, the machine will start to vibrate, eventually thereby destroying itself. In future, research can be conducted to reduce this harmonic distortion by optimizing the rotor and stator pole shapes.

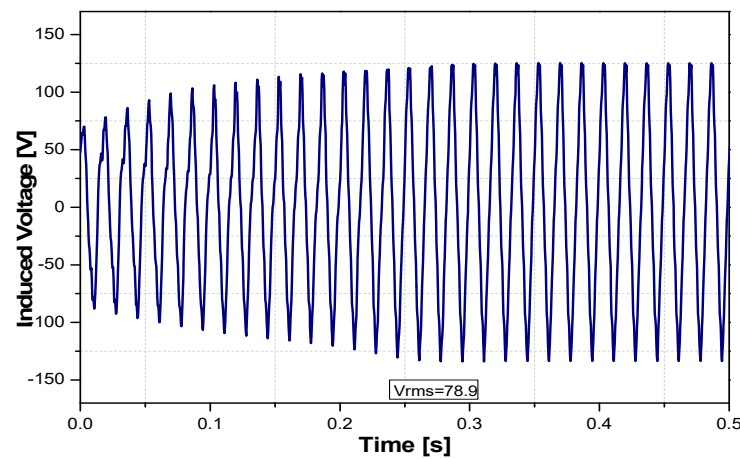


Figure 12. Induced voltage of phase A.

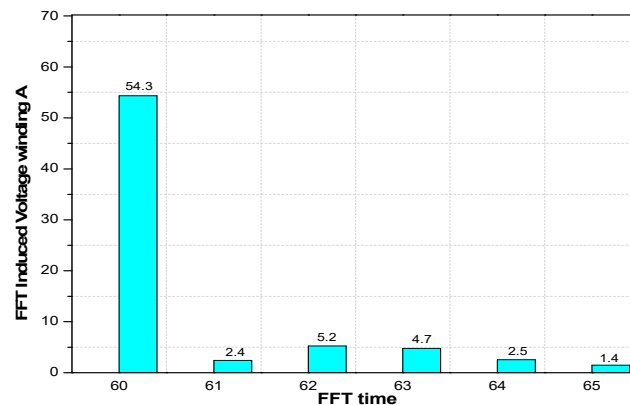


Figure 13. FFT of induced voltage of phase A.

#### 4. Conclusions

This paper introduced a new topology for the brushless wound rotor synchronous machine. The unutilized slots in the already existing topology of [28] are filled up with an additional phase of the rotor harmonic winding. This helps to induce additional currents in the rotor harmonic windings, and hence, the rotor field current from the rotating rectifier circuit is increased. Ultimately, the electromagnetic torque of the proposed topology is increased by 33%. The 2-D FEA analysis was performed and the results have proven the effectiveness of the proposed topology. The improvement in the average torque with the same design parameters helps to increase the torque density of the machine. This will help to make the BL-WRSM suitable for applications where high torque density is required. Torque ripple and the high THD are of slight concern for the machine but these factors can be overcome in future work by employing different optimization techniques.

**Author Contributions:** Conceptualization, Q.A.; methodology, F.A., A.A., Q.A. and A.H.; software, F.A., A.H. and A.A.; validation, A.H., A.I. and M.U.; formal analysis, A.H., M.U. and A.I.; investigation, A.H.; resources, A.I. and M.U.; writing—original draft preparation, F.A., A.H., A.A., A.K. and A.I.; writing—review and editing, A.H., A.I., M.U., A.K. and A.A. All authors have read and agreed to the published version of the manuscript.

**Funding:** This research was funded by Pakistan Science Foundation (PSF) and National Natural Science Foundation of China (NSFC) under the Joint Scientific Exchange Program (JSEP), Project No. PSF-NSFC/JSEP/ENG/S-IBA/05.

**Data Availability Statement:** The original contributions presented in the study are included in the article, further inquiries can be directed to the corresponding author.

**Acknowledgments:** We thank Ghulam Ishaq Khan Institute (GIKI) for their constant support and help. We also want to thank Higher Education Commission (HEC) Pakistan for their support under the project number NRPU-20-14813.

**Conflicts of Interest:** The authors have no conflicts of interest.

## References

1. Shi, Z.; Sun, X.; Cai, Y.; Yang, Z.; Lei, G.; Guo, Y.; Zhu, J. Torque analysis and dynamic performance improvement of a PMSM for EVs by skew angle optimization. *IEEE Trans. Appl. Supercond.* **2019**, *29*, 0600305. [\[CrossRef\]](#)
2. Decker, Ž.; Rudzinskas, V.; Drozd, K.; Caban, J.; Tretjakovas, J.; Nieoczym, A.; Matijošius, J. Analysis of the Vehicle Chassis Axle Fractures. *Materials* **2023**, *16*, 806. [\[CrossRef\]](#) [\[PubMed\]](#)
3. Zhao, F.; Lipo, T.A.; Kwon, B.I. Dual-stator interior permanent magnet vernier machine having torque density and power factor improvement. *Electr. Power Compon. Syst.* **2014**, *42*, 1717–1726. [\[CrossRef\]](#)
4. Kim, B.; Lipo, T.A. Operation and design principles of a PM vernier motor. In Proceedings of the 2013 IEEE Energy Conversion Congress and Exposition, Denver, CO, USA, 15–19 September 2013.
5. Watthewaduge, G.M.A.; Toulabi, M.S.; Filizadeh, S.; Gole, A.M. Performance Analysis and Operating Limits of a Dual-Inverter Open-Winding IPMSM Drive. *IEEE Trans. Energy Convers.* **2019**, *34*, 1655–1666. [\[CrossRef\]](#)
6. Rahman, M.M.; Uddin, M.N. Third Harmonic Injection Based Nonlinear Control of IPMSM Drive for Wide Speed Range Operation. *IEEE Trans. Ind. Appl.* **2019**, *55*, 3174–3184. [\[CrossRef\]](#)
7. Liu, C.; Zhong, J.; Chau, K.T. A Novel Flux-Controllable Vernier Permanent-Magnet Machine. *IEEE Trans. Magn.* **2011**, *47*, 4238–4241. [\[CrossRef\]](#)
8. Wang, H.; Fang, S.; Yang, H.; Lin, H.; Li, Y.; Jiang, J. A Novel Consequent-Pole Hybrid Excited Vernier Machine. *IEEE Trans. Magn.* **2017**, *53*, 8112304. [\[CrossRef\]](#)
9. Atiq, S.; Lipo, T.A.; Kwon, B.I. Experimental verification of winding switching technique to enhance maximum speed operation of surface mounted permanent magnet machines. *IET Electr. Power Appl.* **2016**, *10*, 294–303. [\[CrossRef\]](#)
10. Zhu, Z.Q.; Cai, S. Hybrid excited permanent magnet machines for electric and hybrid electric vehicles. *CES Trans. Electr. Mach. Syst.* **2019**, *3*, 233–247. [\[CrossRef\]](#)
11. Baloch, N.; Atiq, S.; Kwon, B.-I. A Wound-Field Pole-Changing Vernier Machine for Electric Vehicles. *IEEE Access* **2020**, *8*, 91865–91875. [\[CrossRef\]](#)
12. Humza, M.; Yazdan, T.; Siddiqi, M.R.; Cho, H.-W. Brushless Wound Rotor Vernier Motor Using Single-Phase Additional Winding on Stator for Variable Speed Applications. *IEEE Access* **2023**, *11*, 86262–86270. [\[CrossRef\]](#)
13. Zulqarnain, M.; Hammad, S.Y.; Ikram, J.; Bukhari, S.S.H.; Khan, L. Torque Ripple Reduction in Brushless Wound Rotor Vernier Machine Using Third-Harmonic Multi-Layer Winding. *World Electr. Veh. J.* **2024**, *15*, 163. [\[CrossRef\]](#)
14. Lipo, T.A.; Du, Z.S. Synchronous motor drives—a forgotten option. In Proceedings of the 2015 Intl Aegean Conference on Electrical Machines & Power Electronics (ACEMP), 2015 Intl Conference on Optimization of Electrical & Electronic Equipment (OPTIM) & 2015 Intl Symposium on Advanced Electromechanical Motion Systems (ELECTROMOTION), Side, Turkey, 2–4 September 2015; pp. 1–5.
15. Dorrell, D.G. Are wound-rotor synchronous motors suitable for use in high efficiency torque-dense automotive drives? In Proceedings of the IECON 2012—38th Annual Conference on IEEE Industrial Electronics Society, Montreal, QC, Canada, 25–28 October 2012; pp. 4880–4885.
16. Ruuskanen, V.; Niemela, M.; Pyrhonen, J.; Kanerva, S.; Kaukonen, J. Modeling the brushless excitation system for a synchronous machine. *IET Electr. Power Appl.* **2009**, *3*, 231–239. [\[CrossRef\]](#)
17. Yao, F.; An, Q.; Gao, X.; Sun, L.; Lipo, T.A. Principle of Operation and Performance of a Synchronous Machine Employing a New Harmonic Excitation Scheme. *IEEE Trans. Ind. Appl.* **2015**, *51*, 3890–3898. [\[CrossRef\]](#)
18. Nishanth, F.; Khamitov, A.; Severson, E.L. Design of Electric Machine Windings to Independently Control Multiple Airgap Harmonics. *IEEE Trans. Ind. Appl.* **2024**, *60*, 3039–3050. [\[CrossRef\]](#)
19. Yao, F.; An, Q.; Sun, L.; Lipo, T.A. Performance Investigation of a Brushless Synchronous Machine with Additional Harmonic Field Windings. *IEEE Trans. Ind. Electron.* **2016**, *63*, 6756–6766. [\[CrossRef\]](#)
20. Ahmed, S.; Siddiqi, M.R.; Ali, Q.; Yazdan, T.; Hussain, A.; Hur, J. Brushless Wound Rotor Synchronous Machine Topology Using Concentrated Winding for Dual Speed Applications. *IEEE Access* **2023**, *11*, 119560–119567. [\[CrossRef\]](#)
21. Rao, Y.T.; Chakraborty, C.; Basak, S. Brushless Induction Excited Synchronous Generator with Induction Machine Operating in Plugging Mode. *IEEE Trans. Ind. Appl.* **2018**, *54*, 5748–5759. [\[CrossRef\]](#)
22. Ayub, M.; Jawad, G.; Kwon, B. Consequent-pole hybrid excitation brushless wound field synchronous machine with fractional slot concentrated winding. *IEEE Trans. Magn.* **2019**, *55*, 1–5. [\[CrossRef\]](#)
23. Pötter, J.; Pfof, M.; Schullerus, G. Design aspects of a novel brushless excitation system for synchronous machines. In Proceedings of the 2019 IEEE International Electric Machines & Drives Conference (IEMDC), San Diego, CA, USA, 12–15 May 2019; pp. 1228–1233.
24. Ayub, M.; Bukhari, S.S.H.; Jawad, G.; Kwon, B.I. Brushless wound field synchronous machine with third-harmonic field excitation using a single inverter. *Electr. Eng.* **2019**, *101*, 165–173. [\[CrossRef\]](#)

25. Rafin, S.M.S.H.; Ali, Q.; Lipo, T.A. A Novel Sub-Harmonic Synchronous Machine Using Three-Layer Winding Topology. *World Electric. Veh. J.* **2022**, *13*, 16. [[CrossRef](#)]
26. Xu, N.; Sun, X.; Yao, M. Multi-objective optimisation design for brushless electrically excited synchronous machines in electric vehicles. *Int. J. Veh. Des.* **2023**, *92*, 213–235. [[CrossRef](#)]
27. Owuor, J.O.; Munda, J.L.; Jimoh, A.A. An Optimally Controlled Variable Output Wound Rotor Synchronous Machine. *Int. J. Electr. Energy* **2016**, *4*. [[CrossRef](#)]
28. Hussain, A.; Kwon, B.I. A new brushless wound rotor synchronous machine using a special stator winding arrangement. *Electr. Eng.* **2018**, *100*, 1797–1804. [[CrossRef](#)]

**Disclaimer/Publisher’s Note:** The statements, opinions and data contained in all publications are solely those of the individual author(s) and contributor(s) and not of MDPI and/or the editor(s). MDPI and/or the editor(s) disclaim responsibility for any injury to people or property resulting from any ideas, methods, instructions or products referred to in the content.